World Scientific
www.worldscientific.com

Half-Metallic Ferromagnetism in Double Perovskite Ca$_2$CoMoO$_6$ Compound: DFT+U Calculations

A. Djefal[*], S. Amari[*,†,¶], K. O. Obodo[‡], L. Beldi[*], H. Bendaoud[*],
R. F. L. Evans[§] and B. Bouhafs[*]

[*]*Laboratoire de Modélisation et Simulation en Sciences des Matériaux*
Université Djillali Liabès de Sidi Bel-Abbès
Sidi Bel-Abbès 22000, Algeria

[†]*Faculty of Nature and Life Science*
University of Chlef 02000, Algeria

[‡]*Physics Department*
University of South Africa, Pretoria 0001, South Africa

[§]*Department of Physics*
University of York, Heslington, York YO10 5DD, UK
[¶]*siham_amari@yahoo.fr*

A systematic investigation on magnetism and spin-resolved electronic properties in double perovskite Ca$_2$CoMoO$_6$ compound was performed by using the full-potential augmented plane wave plus local orbitals (APW+lo) method within the generalized gradient approximation (GGA-PBE) and GGA-PBE+U scheme. The stability of monoclinic phase ($P2_1/n$ #14) relative to the tetragonal ($I4/m$#87) and cubic ($Fm\bar{3}m$ #225) phase is evaluated. We investigate the effect of Hubbard parameter Uon the ground-state structural and electronic properties of Ca$_2$CoMoO$_6$ compound. We found that the ferromagnetic ground state is the most stable magnetic configuration. The calculated spin-polarized band structures and densities of states indicate that the Ca$_2$CoMoO$_6$ compound is half-metallic (HM) and half-semiconductor (HSC) ferromagnetic (FM) semiconductor with a total magnetic moment of 6.0 using GGA-PBE and GGA-PBE+U, respectively. The Hubbard U parameter provides better description of the electronic structure. Using the Vampire code, an estimation of exchange couplings and magnetic Curie temperature is calculated. Further, our results regarding the magnetic properties of this compound reveal their ferromagnetic nature. The GGA-PBE+U approach provides better band gap results as compared to GGA-PBE approximation. These results imply that Ca$_2$CoMoO$_6$ could be a promising magnetic semiconductor for application in spintronic devices.

Keywords: Density functional theory; spin-polarization; half-metallicity; electronic structure; ferromagnetism; GGA-PBE+U; ordered double perovskite.

[¶]Corresponding author.

1. Introduction

In the last decade, double perovskites $A_2BB'O_6$ (A: Alkali metal, alkaline earth metal or lanthanides) with transition metals at the BB' sites have been extensively studied due to their interesting physical properties, metallicity, half-metallicity, insulating as well as ferromagnetism (FM), anti-ferromagnetism (AFM), ferrimagnetism (FIM), which make them attractive candidates for spintronic applications (like Sr_2FeMoO_6)[1] and magneto-optic devices.[2] This class of materials can exhibit a variety of crystallographic structures for different alkaline and transition metal ions in their lattice. At room temperature, their lattice could be cubic ($Fm\bar{3}m$) as in Ba_2FeMoO_6,[3] tetragonal ($I4/m$) as in Sr_2CoWO_6,[4] monoclinic ($P2_1/n$) as in Ca_2FeMoO_6.[5]

In this family of double perovskites, numerous studies have been carried out on the Ca_2FeMoO_6 system. This system shows ferromagnetism and metallic behavior with high Curie temperature.[5] Recently, $Ca_2Fe_{1-x}Co_xMoO_6$ $(0.1 \leq x \leq 0.4)$ double perovskite compound has been synthesized using the solid-state reaction technique.[6] They showed that with increasing Co concentration, the volume of the lattice increases with the crystal structure unchanged and there is a reduction in the metallicity of the system.

To the best of our knowledge, there are no previous detailed studies using density functional theory to investigate the electronic and magnetic properties for double perovskite Ca_2CoMoO_6 system. We carried out first-principles calculations to investigate the structural stability of Ca_2CoMoO_6 using both the generalized gradient approximation (GGA) and the GGA with the Hubbard Columbic interactions. The Hubbard U correction is introduced to account for the presence of electron–electron correlation associated with the d electrons of the transition metal ions.[7,8] The effect of the Hubbard U (Coulomb interaction correction) on the magnetic behavior and the magnetic properties, which is of interest, is evaluated. We show that the Ca_2CoMoO_6 crystallize in the monoclinic system ($P2_1/n$) using only energetic consideration. The electronic properties are evaluated and an approximation of the magnetic Curie temperature is given.

This study is organized as follows. In Sec. 2, a brief overview of the theoretical method used is presented. The results and discussions are presented in Sec. 3. Finally, the conclusions derived from our calculations are summarized in Sec. 4.

2. Computational Details

Using density functional theory (DFT)[9,10] within both the generalized gradient approximation (GGA-PBE)[11] and (GGA-PBE+U),[12] the total energy of all crystal structures is evaluated. The Hubbard as mentioned above is used to account for the onsite Coulomb interaction. The crystal structure and ionic position were optimized using the full-potential augmented plane wave method (FP-LAPW) as implemented in the WIEN2K code.[13] In the FP-LAPW method, the wave function and potential are expanded using spherical harmonic functions inside the nonoverlapping spheres surrounding the atomic sites (muffin-tin spheres). The Brillouin zone was sampled with a $10 \times 10 \times 7$ k-point mesh and the $R_{MT} \times K_{MAX}$ is set to 8. The muffin-tin (MT) radii of calcium, cobalt, molybdenum and oxygen are set to 2.02, 2.04, 1.75 and 1.55, respectively. To study the electronic and magnetic properties of Ca_2CoMoO_6 crystal structure, the Hubbard U parameter is set to 5 eV and 1 eV for the strongly correlated Co $3d$ electrons[14] and the weakly correlated Mo $4d$ electrons,[15] respectively.

3. Results and Discussion

3.1. *Structural properties and magnetic stability*

To evaluate the most stable phase, the total energy as a function of volume is calculated using GGA-PBE and GGA-PBE+U for the three probable phases [cubic ($Fm\bar{3}m$# 225), tetragonal ($I4/m$# 87) and monoclinic ($P2_1/n$ # 14)] as shown in Fig. 1. Figures 1(a) and 1(b) show that the monoclinic phase is the most stable structure of Ca_2CoMoO_6. Full structural optimization for the double perovskite Ca_2CoMoO_6 compound of the various phases is carried out. The bulk modulus and pressure derivative computed by means of Murnaghan's equation of states[16] using the GGA-PBE and GGA-PBE+U schemes for the three phases are listed in Table 1. To the best of our knowledge, no experimental or *ab-initio* data on the bulk modulus and pressure derivative of Ca_2CoMoO_6 are available in the literature. The calculated lattice parameter obtained is comparable to the work by Poddar *et al.*[6]
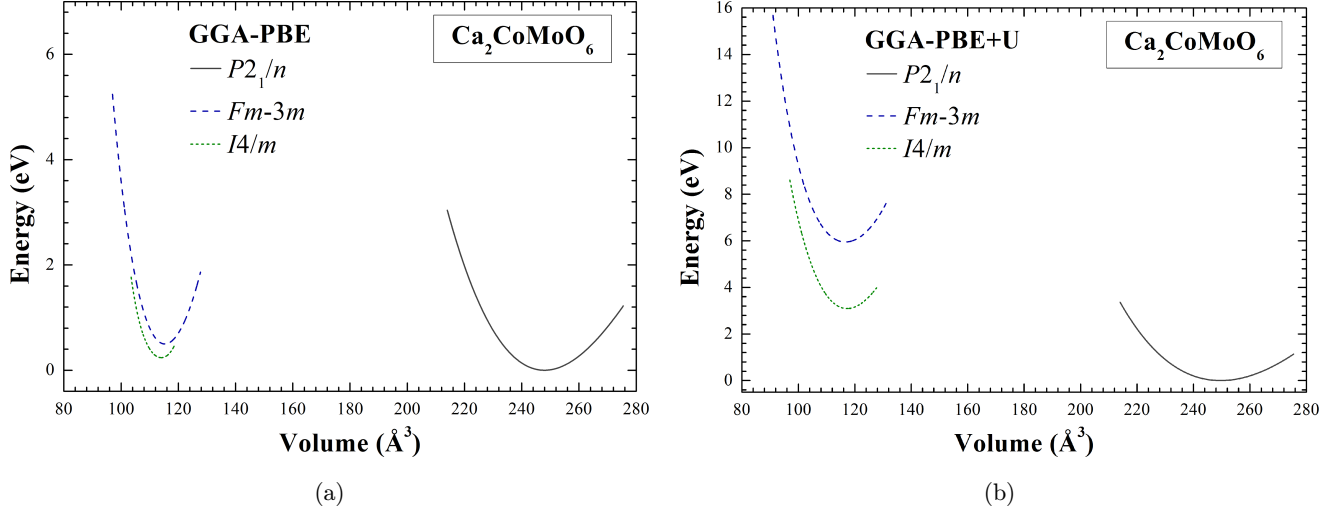
(a)   (b)

Fig. 1. Total energy as a function of volume for the ferromagnetic (FM) spin ordering of Ca_2CoMoO_6 compound in the cubic, tetragonal, and monoclinic structures using (a) GGA-PBE and (b) GGA-PBE+U.

Table 1. The calculated lattice constants (a, b, c in Å, and β in degrees), the bulk modulus B (in GPa) and it's derivative (B') of the Ca_2CoMoO_6 double perovskite structure in $P2_1/n$ monoclinic symmetry with FM ordering obtained using GGA-PBE and GGA-PBE+U approximations.

			a	b	c	β	B	B'
Ca_2CoMoO_6	$P2_1/n$	GGA-PBE	5.55	5.65	7.91	90.2	163	4.38
		GGA-PBE+U	5.56	5.65	7.92	90.2	162	4.45
	$I4/m$	GGA-PBE	5.40	5.40	7.80		184	4.60
		GGA-PBE+U	5.45	5.45	7.88		178	4.45
	$Fm\bar{3}m$	GGA-PBE	7.72	7.72	7.72		201	4.38
		GGA-PBE+U	7.75	7.75	7.75		184	4.52
Ca_2MnMoO_6	$P2_1/n$	Ref. 6	5.41	5.52	7.78	89.91		

The calculated atomic positions for the monoclinic phase are presented in Table 2. The lattice constants obtained within GGA-PBE+U is slightly larger compared to the GGA-PBE approximation.

The monoclinic structure of double perovskite Ca_2CoMoO_6 is optimized for different magnetic spin configurations as shown in Fig. 2. The considered configurations are the ferromagnetic (FM) spin configuration and two independent anti-ferromagnetic (AFM) spin configurations. The two AFM configurations are AFM1 and AFM2, which have both Co and Mo in the AFM coupling along the c

Table 2. The Wyckoff positions of the double perovskite Ca_2CoMoO_6 compound in the monoclinic structure.

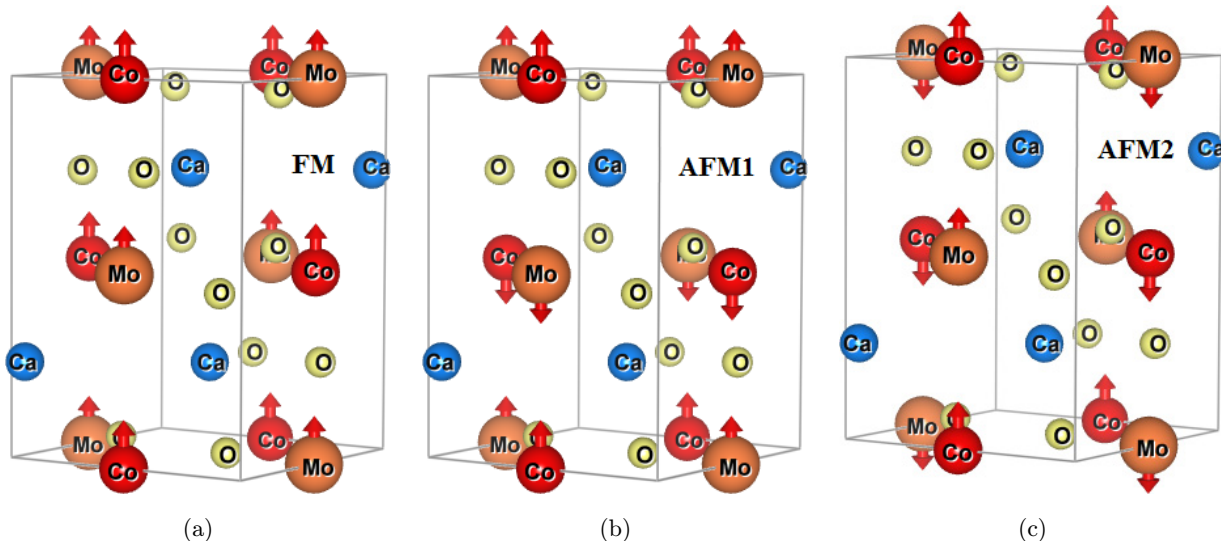|		Site	Ca 4e	Co 2c	Mo 2d	O (1) 4e	O (2) 4e	O (3) 4e
Present work	GGA-PBE	x	0.0110	0.5	0	0.2842	0.3090	0.9116
		y	0.0531	0	0.5	0.3024	0.2797	0.4699
		z	0.2548	0	0	0.0422	0.4488	0.2382
	GGA-PBE+U	x	0.0119	0.5	0	0.2829	0.3135	0.9065
		y	0.0535	0	0.5	0.3070	0.2806	0.4664
		z	0.2543	0	0	0.0444	0.4452	0.2355

Fig. 2. Schematic representation of (a) ferromagnetic FM and the anti-ferromagnetic (b) AFM1, and (c) AFM2 spin configurations of Ca_2CoMoO_6 crystal structure in the monoclinic phase produced by VESTA.[20]

axis. The total energy as a function of the volume for all the considered magnetic configurations in the monoclinic phase using GGA-PBE and GGA-PBE+U is presented in Figs. 3(a) and 3(b). The FM ordering is found to be stable compared to the AFM1 and AFM2 ordering using GGA-PBE. The stability of the FM configuration increases compared to the (AFM1 and AFM2) configurations using the GGA-PBE+U approximation. This shows that the Ca_2CoMoO_6 monoclinic structure exhibits ferromagnetic behavior with possible application as a spintronic material.

3.2. *Electronic structure*

The electronic band structure and density of states of the stable monoclinic ferromagnetic Ca_2CoMoO_6 are calculated within GGA-PBE and GGA-PBE+U approximations. According to Fig. 4(a), the calculated band structure of Ca_2CoMoO_6 compound using GGA-PBE exhibit an indirect band gap $Eg^{Y-D} = 1.58$ eV in the spin up channel. On the other hand, there is a considerable overlap of the valence and conduction bands at the Fermi level in the spin down channel as shown in Fig. 4(b). This implies that the system is half-metallic (HM).
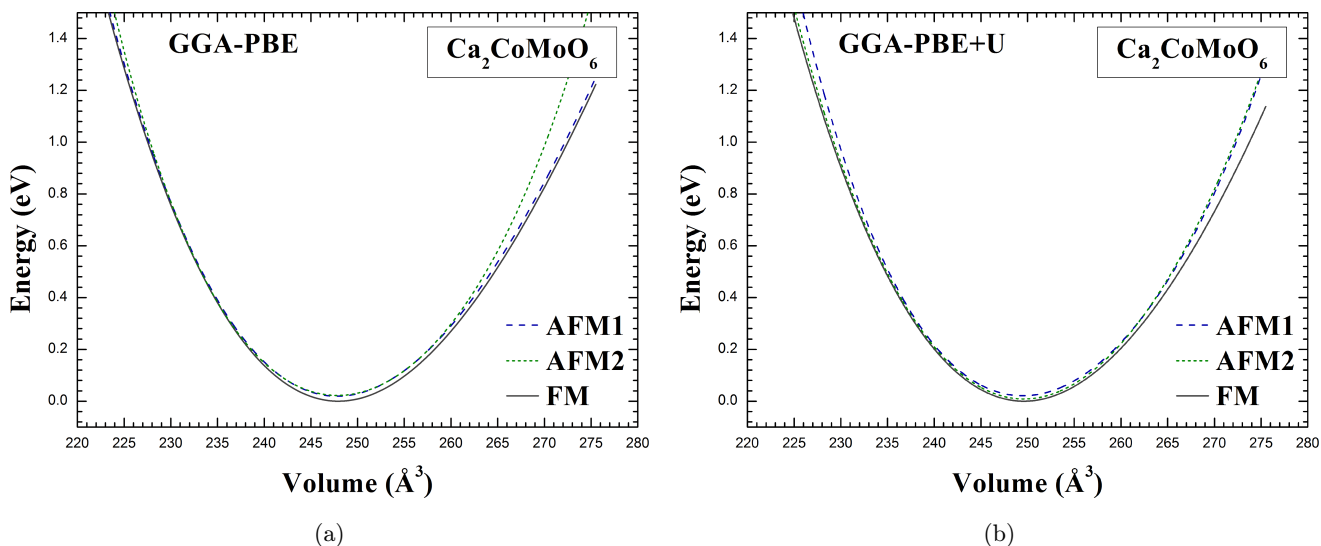

Fig. 3. Total energy as a function of volume for the ferromagnetic (FM) and anti-ferromagnetic [AFM1 and AFM2] spin orderings of the monoclinic Ca_2CoMoO_6 compound using (a) GGA-PBE and (b) GGA-PBE+U.
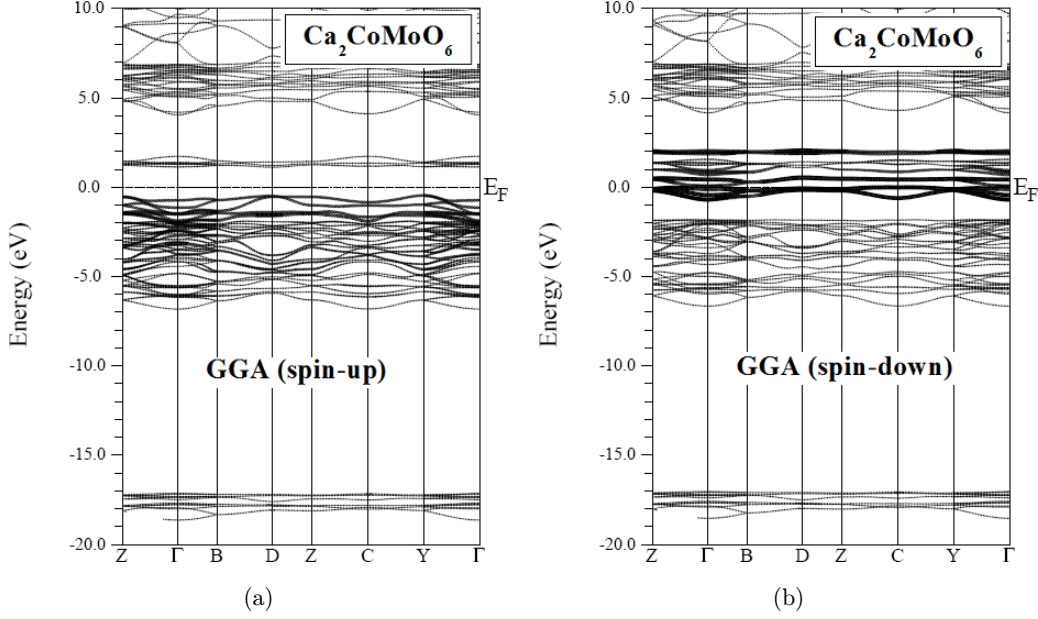
Fig. 4. The calculated spin-polarized band structures (a) spin up and (b) spin down at the equilibrium lattice constant of the monoclinic double perovskite Ca₂CoMoO₆ compound using GGA-PBE. The horizontal dashed line indicates the Fermi level.

Table 3. The calculated total magnetic moment μ_{tot} (in μ_B/Cell) per cell and the local magnetic moments μ_{Co}, μ_{Mo} (in μ_B/atom) of Co, and Mo atoms, respectively, the energy band gaps E_g (spin ↑) and E_g (spin ↓) (in eV) for the majority and minority spin channels, respectively, the half metallic gap E_g^{HM} (in eV), and the half semiconductor gap E_g^{HSC} (in eV) using GGA-PBE and GGA-PBE+U, respectively.

	μ_{Total}	μ_{Co}	μ_{Mo}	E_g (spin ↑)	E_g (spin ↓)	E_g^{HM}	E_g^{HSC}	
GGA-PBE	6	2.57	0.01	1.58	Metal	0.465		HM
GGA-PBE+U	6	2.76	0.02	2.25	1.98		1.98	HSC

This result confirms the half-metallic character of this compound, with a value of the half-metallic gap $Eg^{\text{HM}} = 0.465$ eV and an integer magnetic moment (see Table 3).

To properly ascertain the computed electronic structure, the GGA-PBE+U approximation is carried out. From Fig. 5, the band structure calculated for Ca₂CoMoO₆ using GGA-PBE+U in the monoclinic structure has an indirect gap $E^{Y-\Gamma} = 2.25$ eV in the spin up channel (Fig. 5(a)), and another indirect gap $E^{Y-\Gamma} = 1.98$ eV in the case of the spin down channel (Fig. 5(b)). We find that the spin down channel of the band dispersion has a smaller insulating gap compared to the spin up channel as shown in Figs. 5(a) and 5(b). Hence, the true ground state of Ca₂CoMoO₆ is half-semiconducting (HSC). This result confirms the half-semiconductor nature

of this compound in this structure when using GGA-PBE+U, with a half-semiconductor band gap $E_g^{\text{HSC}} = 1.98$ eV and an integer magnetic moment (see Table 3).

In Figs. 6(a) and 6(b), we present the calculated spin polarized density of states of Ca₂CoMoO₆ using GGA-PBE and GGA-PBE+U. The electronic structure obtained from the DOS using GGA-PBE shows a HM character consistent with our calculated band structure as presented in Fig. 6(a). The O $2p$ orbital extends from about -6.5 eV to -1.2 eV and hybridizes with the Co $3d$ orbitals in the same energy region. The Mo $4d$ orbitals extend from the 1.6–2.5 eV in the conduction band. The band gap within the GGA appears in the spin-up channel. In the spin-down channel, the Co $3d$ states dominate at the Fermi level from
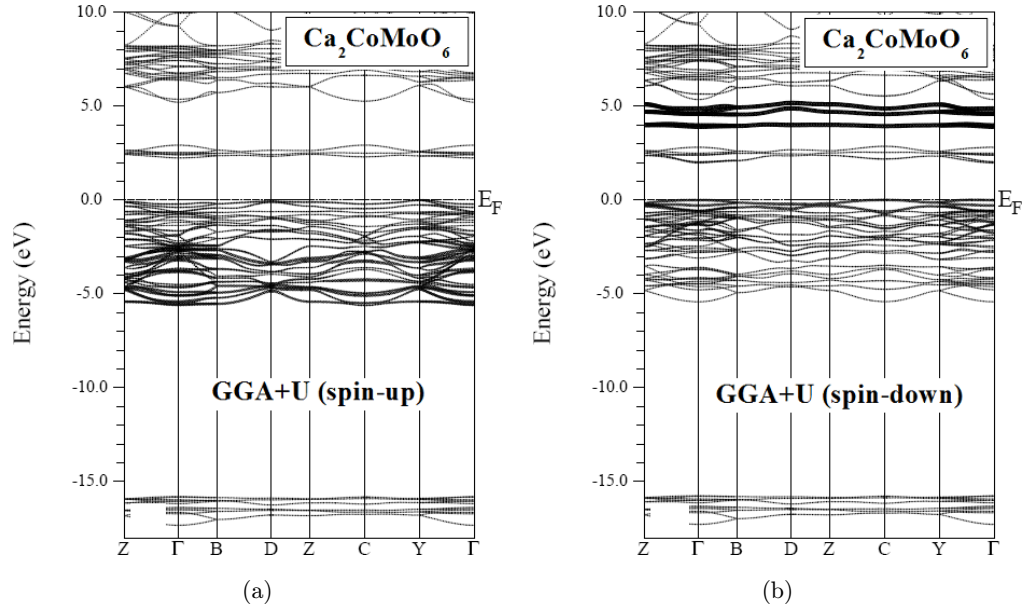
Fig. 5. The calculated spin-polarized band structures (a) spin up and (b) spin down at the equilibrium lattice constant of the monoclinic double perovskite Ca_2CoMoO_6 compound using GGA-PBE+U. The horizontal dashed line indicates the Fermi level.

-0.5 eV to 0.1 eV. Hence, we find that within the GGA-PBE, Ca_2CoMoO_6 is HM.

As mentioned above to account for strong electron–electron correlation in the system, the

electronic structure using GGA-PBE+U is evaluated as shown in Fig. 6(b). The valence band consists purely of Co $3d$ orbitals close to the Fermi level with hybridization of the Mo $4d$, O $2p$, and Co $3d$ in
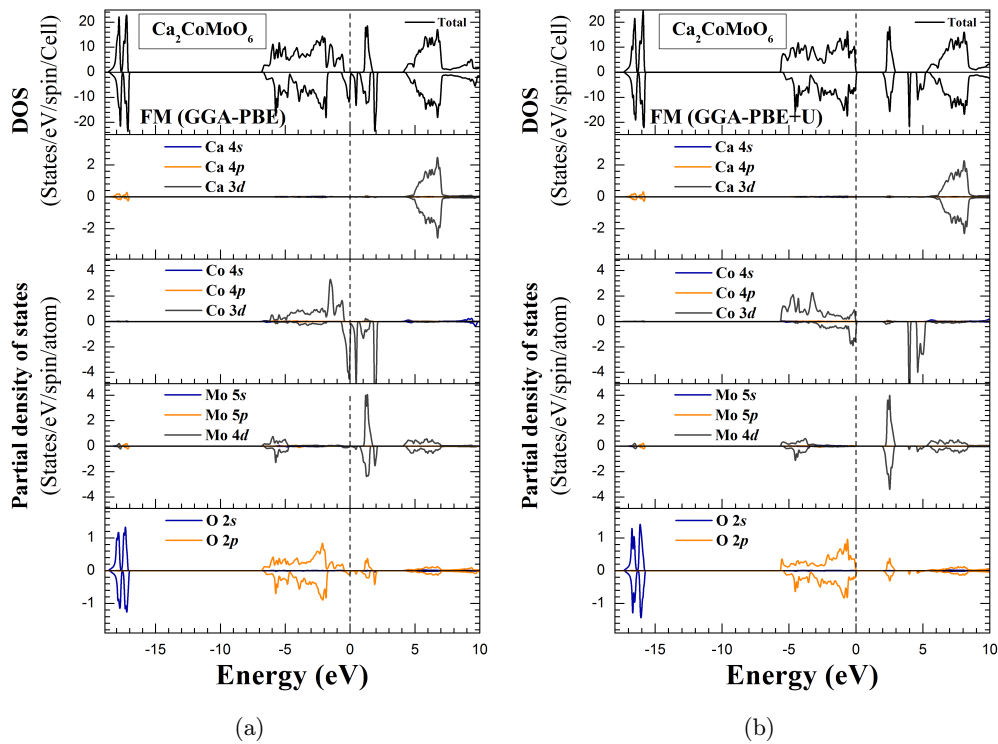

Fig. 6. The calculated spin-polarized total and partial DOS of the monoclinic double perovskite Ca_2CoMoO_6 compound using (a) GGA-PBE and (b) GGA-PBE+U. The vertical dashed line indicates the Fermi level. The positive and negative values of DOS represent the spin-up and spin-down states, respectively.

the spin down channel. We find that using GGA-PBE+U, Ca$_2$CoMoO$_6$ compound presents a half-semiconducting state with integer total magnetic moment arising mainly from Co and a weak magnetic moment from Mo.

To provide further clarification on the half-semiconductor (HSC) nature of Ca$_2$CoMoO$_6$ compound, the spin up and spin down resolved band structure along the high symmetry point in the Brillouin zone and total density of states is presented for the GGA-PBE+U calculation in Fig. 7. Considering the electronic band structure, it is obvious that the half-semiconductor band gap (E_g^{HSC}) is attributed to the spin down states. The top of the valence bands in the spin up and spin down resolved band structures are nearly at the same level, whereas the bottom of the conduction bands show different values at the Γ-point, given a difference band gap value $\Delta E_g = E_g$ (spin $\uparrow$) $- E_g$ (spin $\downarrow$) $= 0.25$ eV. The density of states calculation affirms this assertion as shown on the right side of Fig. 7.

The calculated magnetic properties using GGA-PBE and GGA-PBE+U are summarized in Table 3. We show the total and individual magnetic moments of the atoms per unit cell of Ca$_2$CoMoO$_6$. The total magnetic moment of Ca$_2$CoMoO$_6$ arises mainly from the Co atoms with a weak additional contribution of Mo, Ca and O atoms as mentioned above.

3.3. *Exchange couplings and magnetic Curie temperature*

The Curie temperature of a magnetic material is defined principally by the exchange interaction, which determines the alignment of atomic spins, and makes a material ferromagnetic on the macroscopic scale. Vampire software package[17,18] contains a predefined function to calculate the Curie temperature of a material by performing a temperature sweep and calculating the average magnetization, giving the classic (M–T) curve. The exchange energy is calculated from the following expression:

$$H = -\sum_{i \neq j} J_{ij} \hat{S}_i \bullet \hat{S}_j,$$

where J_{ij} is the exchange energy between nearest neighboring spins, and S_i is the spin operator at site i (in both of the Co and Mo sub-lattices). There exists a relation between the magnetic energies e_{ij} and exchange parameter J_{ij}, which can be expressed and estimated as follows:

$$e_{ij} = J_{ij} \hat{S}_i \bullet \hat{S}_j,$$

where S_i takes either $\frac{3}{2}$ and $\frac{1}{2}$ for the Co and Mo spins, respectively. The exchange interactions were obtained by mapping *ab initio* electronic structure calculations to the classical Heisenberg Hamiltonian.[19] From the total energy difference (relative to FM configuration), we obtain the
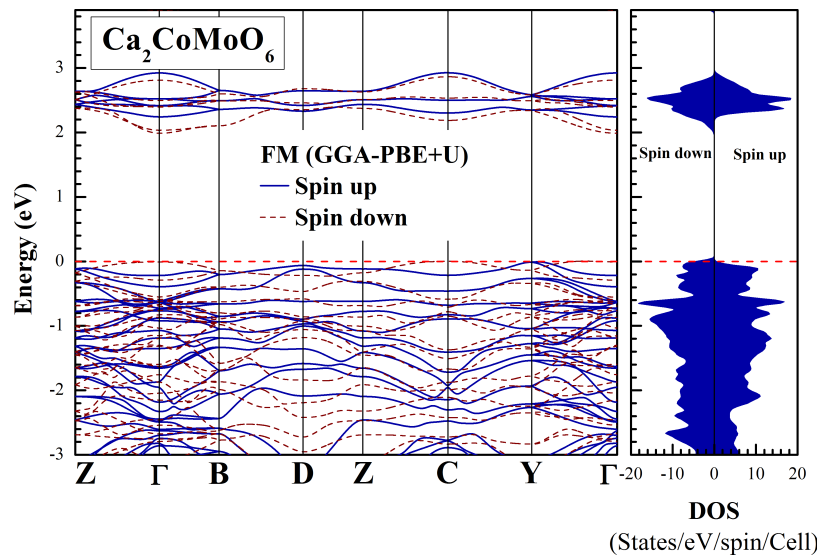

Fig. 7. The calculated spin-polarized band structure and total DOS of the monoclinic double perovskite Ca$_2$CoMoO$_6$ compound in the FM configuration using GGA-PBE+U. The vertical dashed line indicates the Fermi level. The positive and negative values of DOS represent the spin-up and spin-down states, respectively.

Table 4. The calculated spin exchange energies e_{ij} and constants J_{ij} in (meV) of double perovskite Ca_2CoMoO_6 for the nearest-neighbor within GGA-PBE and GGA-PBE $+U$.

| | e_{ij} (meV) | | J_{ij} (meV) | |
	GGA-PBE	GGA-PBE+U	GGA-PBE	GGA-PBE+U
Co–Mo	7.42	9.90	6.89	9.19
Co–Co	−49.08	−21.81	−37.25	−16.55
Mo–Mo	29.27	117	18.87	75.47

following equations from the three magnetic structures by considering only the nearest neighbor:

$$\begin{cases} 0 = 8e_{\text{Co–Mo}} + 3e_{\text{Co–Co}} + 3e_{\text{Mo–Mo}}, \\ E_{\text{AFM1}} - E_{\text{FM}} = -e_{\text{Co–Co}} - e_{\text{Mo–Mo}}, \\ E_{\text{AFM2}} - E_{\text{FM}} = -4e_{\text{Co–Mo}} - e_{\text{Co–Co}}. \end{cases}$$

We solve the e_{ij} parameters from the above equation set, and then calculate the exchange coupling parameters J_{ij} by using the above relations in GGA-PBE and GGA-PBE+U. The spin exchange energies e_{ij} and constants J_{ij} are summarized in Table 4. As can be seen in Table 4, there is a strong qualitative difference in the calculated value of the nearest-neighbor interactions in the two cases: in GGA-PBE and GGA-PBE+U. Starting from FM, we obtain a tendency to retain ferromagnetism (positive exchange constant); while starting from the AFM state, we obtain a tendency to retain anti-ferromagnetism (negative exchange constant). For the more distant neighbors Co–Mo the two

calculations give quantitative, but not so much qualitative, differences. The Co–Mo spin exchange energies is much smaller than the Co–Co and Mo–Mo values using GGA-PBE and GGA-PBE+U. As a result, the spin exchange parameters J_{ij} are 6.89 (GGA-PBE) and 9.19 meV (GGA-PBE+U) between the nearest Co–Mo pair, much smaller than those between Co–Co and Mo–Mo. It is clear that the Co–Co and Mo–Mo spin coupling is dominant over the Co–Mo. The periodic boundary conditions in all three spatial dimensions are set with respectively ($L = 10$ nm, 20 nm and 30 nm). The calculated T_C value is equivalent to 278 K shown in Fig. 8.

4. Conclusion

In summary, using the first-principles FP-LAPW method within GGA–PBE and GGA-PBE+U for the exchange correlation functional, we have investigated the electronic structure and magnetization of Ca_2CoMoO_6 crystal structure. The results indicate that the inclusion of the Hubbard U Coulomb interaction provides better description of the electronic structure. The analysis of the calculated spin-polarized band structures and densities of states indicate that Ca_2CoMoO_6 compound was half-metallic (HM) within GGA-PBE and a half-semiconductor (HSC) ferromagnetic (FM) with a total magnetic moment of 6.0 within GGA-PBE+U. Our Monte Carlo simulations illustrate very high Curie temperatures of 278 K for Ca_2CoMoO_6 crystal structure. The results of the study are useful towards applying Ca_2CoMoO_6 crystal structure as a potential spintronic material.
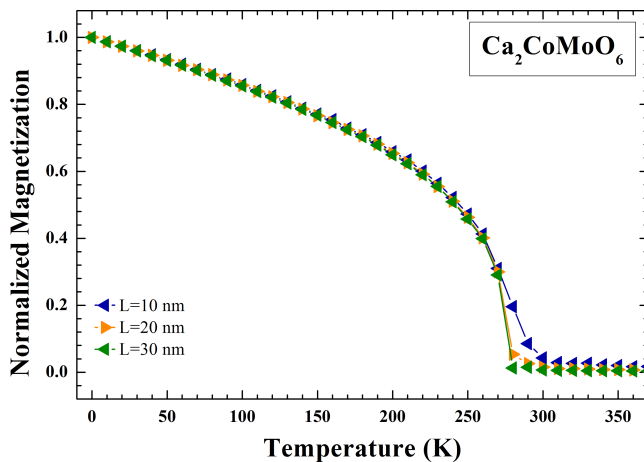

Fig. 8. The temperature dependent magnetization of the monoclinic double perovskite Ca_2CoMoO_6 compound calculated using the atomistic spin model implemented in the Vampire software package.[17,18]

Acknowledgments

References

1. K. I. Kobayashi, T. Kimura, H. Sawada, K. Terakura and Y. Tokura, *Nature* **395**, 677 (1998).
2. Y. Shimakawa, M. Azuma and N. Ichikawa, *Materials* **4**, 153 (2011).
3. C. Ritter, M. Ibarra, L. Morellon, J. Blasco, J. Garcia and J. De Teresa, *J. Phys.: Condens. Matter* **12**, 8295 (2000).
4. M. Viola, M. Martinez-Lope, J. Alonso, J. Martinez, J. De Paoli, S. Pagola, J. Pedregosa, M. Fernandez-Diaz and R. Carbonio, *Chem. Mater.* **15**, 1655 (2003).
5. R. P. Borges, R. M. Thomas, C. Cullinan, J. M. D. Coey, R. Suryanarayanan, L. Ben-Dor, L. Pinsard-Gaudart and A. Revcolevschi, *J. Phys., Condens. Matter* **11**, L445 (1999).
6. A. Poddar, S. Das and B. Chattopadhyay, *J. Appl. Phys.* **95**, 6261 (2004).
7. K. O. Obodo and N. Chetty, *J. Phys., Condens. Matter* **25**, 145603 (2013).
8. K. O. Obodo and N. Chetty, *J. Nucl. Mater.* **442**, 235 (2013).
9. P. Hohenberg and W. Kohn, *Phys. Rev.* **136**, B864 (1964).
10. W. Kohn and L. J. Sham, *Phys. Rev.* **140**, A1133 (1965).
11. J. P. Perdew, K. Burke and Y. Wang, *Phys. Rev. B* **54**, 16533 (1996).
12. V. I. Anisimov, J. Zaanen ans O. K. Andersen, *Phys. Rev. B* **44**, 943 (1991).
13. P. Blaha, K. Schwarz, G. Madsen, D. Kvasnicka and J. Luitz, *An Augmented Plane Wave Plus Local Orbitals Program for Calculating Crystal Properties* (Vienna University of Technology, Austria, 2012).
14. W. Pickett, S. Erwin and E. Ethridge, *Phys. Rev. B* **58**, 1201 (1998).
15. D. Sarma, P. Mahadevan, T. Saha-Dasgupta, S. Ray and A. Kumar, *Phys. Rev. Lett.* **85**, 2549 (2000).
16. F. D. Murnaghan, *Proc. Natl. Acad. Sci.* **30**, 244 (1944).
17. R. F. L. Evans, W. J. Fan, P. Chureemart, T. A. Ostler, M. O. Ellis and R. W. Chantrell, *J. Phys.: Condens. Matter* **26**, 103202 (2014).
18. R. F. L. Evans, U. Atxitia and R. W. Chantrell, *Phys. Rev. B* **91**, 144425 (2015).
19. A. Liechtenstein, V. Anisimov and J. Zaanen, *Phys. Rev. B* **52**, R5467 (1995).
20. K. Momma and F. Izumi, *J. Appl. Crystallogr.* **41**, 653 (2008).